transport through the freeboard of a gas solid fluidized bed," *Fluidization*, Proc. of 3rd Found. Conf. on Fluidization, Plenum Publication, England, Eds., Grace and Master (1980).
Kunii, D., and O. Levenspiel, "Fluidization engineering," Robert E. Krieger Publishing Co., Huntington, NY (1977).
Leva, M., "Elutriation of fines from fluidized systems," *Chem. Eng. Prog.*, **47**, No. 1, 39 (1951).
Leva, M., and C. Y. Wen, "Elutriation," *Fluidization*, Eds., J. F. Davidson and D. Harrison, Chap. 14, Academic Press, New York (1971).
Levy, Y., "Development of an LDA technique for two phase flows in the freeboard of a fluidized bed," (1982).
Lewis, W. K., E. R. Gilliland, and P. M. Lang, "Entrainment from fluidized beds," *Chem. Eng. Prog. Symp. Ser.*, **58**, No. 38, 65 (1962).
Lin, L., J. T. Sears, and C. Y. Wen, "Elutriation and attrition of char from a large fluidized bed," *Powder Tech.*, **27**, 105 (1980).
Merrick, D., and J. Highley, "Particle size reduction and elutriation in a fluidized bed process," *AIChE Symp. Ser.*, **70**, No. 137, 366 (1972).
Thomas, W. J., P. J. Grey, and S. B. Watkins, "Effect of particle size distribution in fluidization," *British Chem. Eng.*, 176 (1961).
Ungut, A., A. J. Yule, D. S. Taylor, and N. A. Chigier, "Simultaneous velocity and particle size measurements in two-phase flow by laser anemometry," AIAA 16th Aerospace Sciences Meeting, Huntsville, AL (Jan. 16–18, 1978).
Wen, C. Y., and R. F. Hashinger, "Elutriation of solid particles from a dense-phase fluidized bed," AIChE J., **6**, No. 2, 220 (1960).
Werther, J., and O. Moulerus, "The local structure of gas fluidized beds. II: The spatial distribution of bubbles," *Int. J. Multiphase Flow*, **1**, 123 (1973).
Zenz, F. A., and N. A. Weil, "A theoretical-empirical approach to the mechanism of particle entrainment from fluidized bed," *AIChE J.*, **4**, 4 (1958).

Manuscript received June 1, 1982; revision received December 10, and accepted December 14, 1982.

Convective Diffusional Deposition and Collection Efficiency of Aerosol on a Dust-Loaded Fiber

A three-dimensional stochastic model, which is effective for the convective diffusional deposition of aerosol particles, was developed starting from Langevin's equation. The model was utilized to simulate collection and agglomeration processes of particles on a cylindrical fiber. By obtaining the distribution of captured particles on a fiber and the evolution of the collection efficiency of a dust-loaded fiber through the simulation, the effect of Peclet number, interception parameter, and the accumulated mass of particles on them were discussed. Further, the collection efficiency of a dust-loaded fiber was correlated by using a linear function of the accumulated mass of particles in a unit filter volume. Dependence of coefficient in the linear function, collection efficiency raising factor on Peclet number, and interception parameter were also discussed.

CHIKAO KANAOKA and HITOSHI EMI
Department of Chemical Engineering
Kanazawa University
Kanazawa, Japan

and

WIWUT TANTHAPANICHAKOON
Department of Chemical Engineering
Chulalongkorn University
Bangkok, Thailand

SCOPE

Fibrous air filter is composed of various kinds of fine fibers and is capable of collecting fine particles efficiently; the pressure drop across the filter is not so high because of low packing density of the filter. Hence, fibrous air filter is used to purify the air of particles. However, since it is usually operated for a long range of time, it is evident that the fibers in it are more or less covered with collected particles so that the filtering characteristic alters with time. Therefore, it is necessary for the rational design and operation of a filter to know the performance of a dust-loaded filter.

There are few available data and theories on a dust-loaded filter, although enormous number of studies have been done on a clean filter where no particles are captured on the fibers in it. Consequently, fibrous air filter has been designed and operated based on designer's or operator's own experiences or knowhow.

Once aerosol particles are captured on fibers in a filter, they change flow pattern around the fibers, thus affecting the filtering characteristic of the upcoming particles. As a result, they build up particle agglomerates on the fibers with random sizes, shapes and distributions. This was the main reason why the filtering performance of a dust-loaded filter has not been studied for a long time, despite the advance in the filtration theory for a clean filter. However, we know that filter performance does not change so much for a long period of time, if the collection efficiency of the filter is not so good or the aerosol concentration is very low. On the contrary, if the collection efficiency of the filter is high or particle concentration is high, it changes rapidly with operation period. Filter structure and filtration condition also affect the filter performance. These facts suggest that the filter performance is closely related to the dust load in the filter and filtration conditions. Hence, if the collection efficiency of a single fiber with dust load is expressible by some measurable or predictable parameters, the collection efficiency of a filter at arbitrary operation period and conditions can be evaluated.

In this paper, a simple simulation method, using Monte Carlo simulation technique to estimate the growing process of particles dendrites on a fiber by convective Brownian diffusion was proposed. Then, single fiber collection efficiency was evaluated using the simulation results. Finally, it was correlated with the accumulated mass of particles in a filter.

CONCLUSIONS AND SIGNIFICANCE

The proposed three-dimensional stochastic model for the simulation of the collection and agglomeration processes of particles on a fiber was found to be effective for the analysis of the convective diffusional deposition of aerosol particles on a dust-loaded fiber.

The model predicted the deposition of particles on the rear surface of a fiber and the appearance of the maximum deposition of particles at a certain angle from the front stagnation point. The latter was observed in the case of inertia and/or interception but the former was not. The angle of the maximum deposition shifted to larger angle as interception parameter $R(=D_p/D_f)$ decreased and as $Pe(=D_f u_0/D_{BM})$ increased, where D_f and D_p are the fiber and the particle diameters; D_{BM} stands for the Brownian diffusivity of a particle; and u_0 denotes the filtration velocity. The peak position at pure interception was found to be the asymptotic position for the case of $Pe = \infty$. The predicted distribution agreed with the previous experimental observations.

Based on the simulation results, the collection efficiency of a dust-loaded fiber was calculated for various combinations of Pe and R, and was found to conform with the previously reported theory at no dust load on a fiber but to increase with the accumulated mass of particles on the fiber regardless of filtration conditions. The collection efficiency was then correlated with the accumulated mass of particles in a unit filter volume and was found to be expressible by the following linear function even for the case of diffusion-interception collection of particles as well as for the case of inertia interception.

$$\eta_{DIM}/\eta_{DI} = 1 + \lambda m$$

The coefficient in the linear function, collection efficiency raising factor, which indicates the degree of the increasing rate of collection efficiency with dust load, varied from 0.8 to 15 and 0.6 to 3.1 for R = 0.1 and 0.2, respectively, when Pe ranged from 200 to infinity.

INTRODUCTION

It is now known that accumulated mass of particles in a fibrous air filter remarkably enhances the collection efficiency, regardless of collection mechanisms. Several experimental studies (Kimura et al., 1964; Billings, 1966; Yoshioka et al., 1969) have found that the collection efficiency and the pressure drop of a fibrous air filter do vary with operating time.

Deterministic model (Payatakes et al., 1976a, 1976b, 1976c, 1977, 1979) and stochastic ones (Tien et al., 1977; Wang et al., 1977; Beizaie et al., 1979; Kanaoka et al., 1978, 1980a, 1980b) have been developed to study the deposition of aerosol particles by inertia and/or interception. Recently, Payatakes et al. (1980b) have extended their model to convective diffusional deposition.

Capable of predicting the relevant phenomena well while relying on basic physical principles, both types of models have their own advantages and disadvantages. Though they have to resort to numerical solutions, the deterministic approach generally consumes less computer time than the stochastic one. This is because the former approach was primarily interested in investigating the mean behavior or characteristics of the phenomena. Since it is virtually impossible to simulate every detail of the tremendously large number of collisions experienced by each aerosol particle during its flight around a fiber, the present stochastic model relied on the theory of Brownian motion.

What follows is a mathematical description of the model, and an explanation of the procedure of Monte Carlo simulation and a presentation and discussion of the major results for convective diffusional deposition obtained under various filtration conditions.

STOCHASTIC MODEL

The starting point of the model is the Langevin's equation for a fine particle moving along an air stream with air velocity u:

$$\frac{dv}{dt} = -\beta(v - u) + A(t) \tag{1}$$

For an adequately short time period t in which u remains essentially constant, Eq. 1 can be rewritten as

$$\frac{dw}{dt} = -\beta w + A(t) \tag{2}$$

where $w = v - u$ is the particle velocity relative to u. Thus, as long as the time scale of interest Δt is adequately larger than the relaxation time β^{-1}, all results pertaining to the theory of Brownian motion are applicable (Uhlenbeck et al., 1930; Doob, 1942; Chandrasekhar, 1943; Wang et al., 1945).

In this case, the probability distribution for the position vector r_i of a particle at time $t + \Delta t$, with previous values w_{i-1} and r_{i-1} at time t, is a three-dimensional normal distribution with $\sigma_x = \sigma_y = \sigma_z = \sigma = \sqrt{2D_{BM}\Delta t}$, namely,

$$W(r_i,\Delta t;w_{i-1},r_{i-1}) = \frac{1}{(4\pi D_{BM}\Delta t)^{3/2}}\exp(-|r_i - r_{i-1}|^2/4D_{BM}\Delta t) \text{ for } t \gg \beta^{-1} \tag{3}$$

This means that the Brownian movement of a fine particle relative to the air flow can be simulated by the difference equation.

$$r_i = r_{i-1} + \sigma n_{i-1} \quad (i = 1,2,3,\text{- - - -}) \tag{4}$$

where $n = (n_x,n_y,n_z)$ is a standard normal random vector with zero mean and standard devication $\sigma = \sqrt{2D_{BM}\Delta t}$. Since the effect of convection would have caused the particle to move an additional distance $u_{i-1}\Delta t$, Eq. 4 can be rewritten as

$$P_i = P_{i-1} + u_{i-1}t + \sigma n_{i-1} \tag{5}$$

Since all physical parameters like the local air velocity u can be treated as constant during each subinterval Δt by using dimensionless variables; $P = p/(D_f/2)$, $U = u/u_0$, and $\tau = tu_0/(D_f/2)$, Eq. 5 is made dimensionless as

$$P_i = P_{i-1} + U_{i-1}\Delta\tau + 2\sqrt{\frac{\Delta\tau}{Pe}}n \tag{6}$$

Procedure of Monte Carlo Simulation

Figure 1 is the schematic diagram of a representative fiber surrounded by Kuwabara's cell. The flow in the cell was given by the following equation (Kuwabara, 1959).

$$\psi = \frac{y}{2\kappa}\left[\left(1 - \frac{\alpha}{2}\right)\frac{1}{x^2 + y^2} - (1 - \alpha) + ln(x^2 + y^2) - \frac{\alpha}{2}(x^2 + y^2)\right] \tag{7}$$

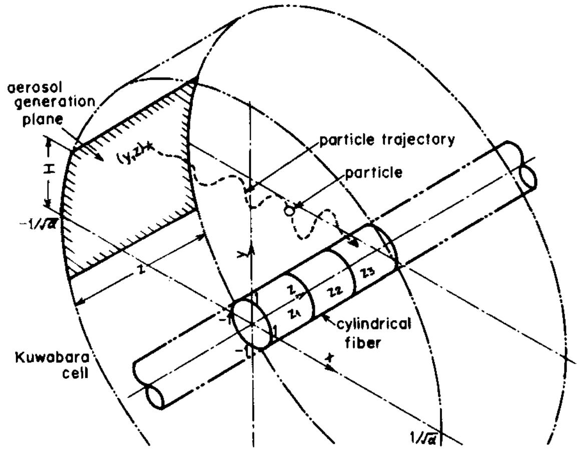

Figure 1. Schematic diagram of Kuwabara's cell.

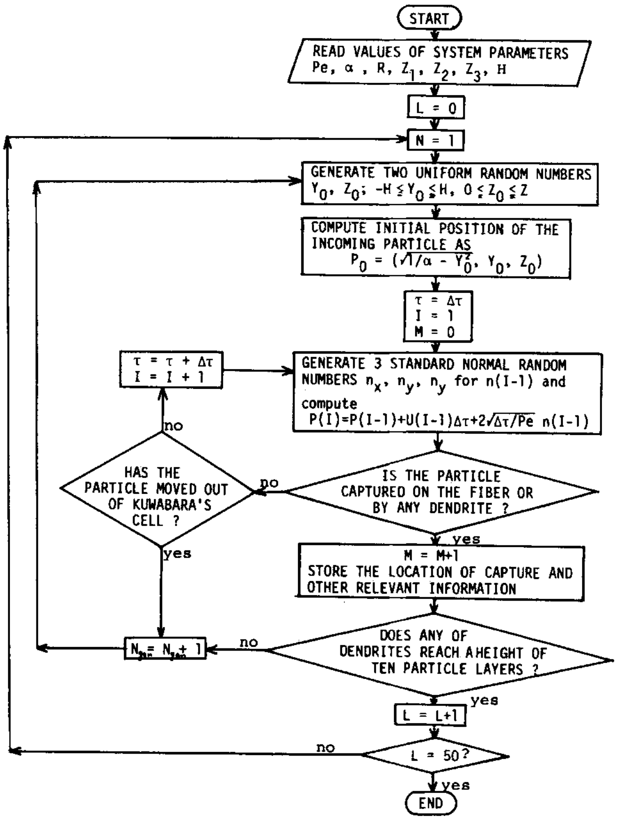

Figure 2. Flow chart of simulation procedure.

where,

$$\kappa = -\ln\alpha + \alpha - \frac{\alpha^2}{4} - \frac{3}{4} \tag{8}$$

The velocity vector U is then

$$U = (u_x, u_y, u_z) = (\partial\psi/\partial y, -\partial\psi/\partial x, 0) \tag{9}$$

Furthermore, the radius R_c of the cylindrical cell, within which Eqs. 6 through 9 are valid, was related to the packing density α by:

$$R_c = 1/\sqrt{\alpha} \tag{10}$$

Using Kuwabara's flow field, simulation was carried out according to the following procedure.

1) The initial position P_0 of an incoming particle was chosen randomly on the generation plane, which overlaps the cell surface and has height $2H$ and width Z (hatched area in Figure 1). Specifically, two mutually independent uniform random numbers, y_0 and z_0, $(-H \leqq y_0 \leqq H,\ 0 \leqq z_0 \leqq Z)$, were generated using subroutine RANDOM (Tanthapanichakoon, 1978) to give $P = (-\sqrt{1/\alpha - y_0^2}, y_0, z_0)$, since we must have $x_0^2 + y_0^2 = 1/\alpha$ on the generation plane.

2) The convective Brownian movement of the particle during successive time steps was simulated consecutively using Eqs. 6 through 9. At each time step, three mutually uncorrelated standard normal random numbers, n_x, n_y and n_z were generated using subroutine RND (Tanthapanichakoon, 1978) and utilized as the components of n_{i-1} in Eq. 6.

3) The new position vector P_i at the end of the each time step was checked to see whether it had collided on the fiber surface or with any of the previously captured particles.

4) Otherwise, Steps 2 and 3 were repeated until it either was captured or had moved out of the rear boundary of the cell.

5) Steps 1 to 4 were repeated until one of the dendrites grew up to a predetermined height of ten particle layers. This represented one sample or one record of Monte Carlo simulation.

6) Steps 2 to 5 were repeated a number of times to yield enough informations for stochastic analysis.

Time step $\Delta\tau$ and fiber length Z are the two most important parameters that control the accuracy and computer time of the present simulation. A shorter time step and a longer fiber length would enhance accuracy but consume disproportionately longer computer time. In this study, their proper values were determined heuristically through simulation of particle deposition for the case of $Pe = 200$ and $R = 0.1$. Results were listed in Table 1. For the cases of Run 1 to 3, simulations were carried out in the upper hemicylinder of Kuwabara's cell and rebound of aerosol particles on both end walls of test fiber and horizontal plane was allowed; but in other cases, simulations were carried out in the full cylinder of the cell and no rebound was allowed. Hence, obtained results by both methods are not comparable directly with each other. The effect of $\Delta\tau$ was probed from the results of Run 1 to 3. Obviously, collection efficiency and computer time decrease as $\Delta\tau$ increases.

TABLE 1. EFFECT OF $\Delta\tau$ AND Z_2 ON OVERALL COLLECTION EFFICIENCY FOR THE CASE OF $Pe = 200$ AND $R = 0.1$

Run No.	$\Delta\tau$	Z_1	Z_2	Z_3	Z	η**	CPU Time
1*	0.08	—	1	—	1	0.269	220.1
2*	0.5	—	1	—	1	0.255	48.1
3*	2.0	—	1	—	1	0.228	18.0
4	0.5	1	0.8	1	2.8	0.110	154.8
5	0.5	1	0.8	1	2.8	0.122	205.2
6	0.98	1	0.8	1	2.8	0.119	90.6
7	0.98	1	0.8	1	2.8	0.124	117.9
8	2.0	1	0.8	1	2.8	0.127	57.5
9	0.5	1	1.6	1	3.6	0.123	199.2
10	2.0	1	1.6	1	3.6	0.122	53.7
11	2.0	1	1.6	1	3.6	0.138	89.0

* Simulation was carried out in the upper hemicylinder of Kuwabara's cell with bouncing of aerosol particles on side walls and horizontal plane.
** Efficiency shown here is simply given by the ratio of the number of captured particles to total income particles.

TABLE 2. SIMULATION CONDITIONS

Interception Parameter R[—]	0.1,0.2
Peclet Number Pe[—]	200,1000,5000
Packing Density of Filter α[—]	0.03
Length of Test Fiber Section I Z_1[—]	1.0
II Z_2[—]	1.6
III Z_3[—]	1.0
Half Height of Generation Plane H[—]	2.0
Number of Simulation L[—]	50

However, the difference in efficiency between $\Delta\tau = 0.08$ and 0.5 is much smaller than that between $\Delta\tau = 0.5$ and 2.0. Hence, $\Delta\tau = 0.5$ was adopted in this work. Next, the effect of fiber length was tested. In this consideration, the entire fiber length Z was divided into three subsections, 1, 2 and 3, of length Z_1, Z_2 and Z_3. Furthermore, to offset end effect, generation of particles took place over the entire length Z, and Z_2 was flanked by two relatively wide buffer zones Z_1 and Z_3. In this way, the shapes of dendrites within

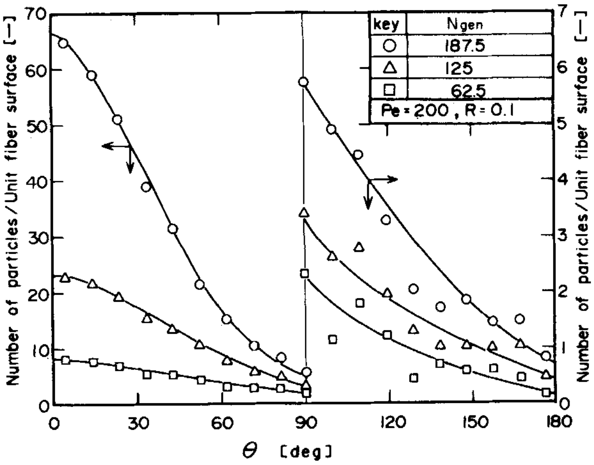

Figure 3. Angular distribution of number of deposited particles on a fiber for the case of Pe = 200 and R = 0.1.

TABLE 3. SIMULATION RESULT OF DENDRITE GROWTH ON A FIBER FOR THE CASE OF Pe = 200 AND R = 0.1

M	r	θ	z	N**	M	r	θ	z	N**
1	1.1	78.1	0.838	100	51	1.1	3.6	0.316	3
2*	1.1	245.4	1.092	5	52	1.475	347.5	1.096	7
3	1.1	71.2	1.240	50	53	1.263	303.3	0.475	11
4	1.1	321.4	1.470	7	54	1.194	341.8	0.119	38
5	1.1	31.1	1.469	12	55*	1.266	121.4	0.901	42
6	1.183	25.9	1.320	19	56	1.245	297.5	0.990	19
7	1.212	315.4	1.355	26	57	1.1	41.3	0.507	6
8	1.1	298.0	1.127	39	58	1.346	49.1	1.293	4
9*	1.1	243.6	0.333	48	59	1.379	352.2	0.965	11
10	1.1	286.6	0.461	83	60	1.280	39.8	0.425	56
11	1.1	333.1	1.456	2	61	1.246	16.9	1.332	8
12	1.211	299.4	1.176	147	62	1.536	47.8	1.242	51
13	1.397	302.6	0.119	139	63	1.386	303.7	0.987	3
14	1.235	70.8	0.843	78	64	1.676	49.7	1.375	24
15	1.1	344.5	1.493	31	65	1.278	2.8	1.084	6
16	1.1	318.0	1.165	8	66	1.343	322.2	1.369	43
17	1.1	91.4	0.110	14	67	1.202	33.9	0.293	25
18	1.438	310.4	0.088	13	68*	1.1	152.7	1.292	27
19	1.1	334.7	0.013	7	69	1.424	351.5	0.077	35
20	1.1	345.4	0.552	12	70	1.223	16.7	0.643	68
21	1.311	316.6	0.045	22	71	1.549	349.9	0.227	2
22	1.421	323.6	0.037	48	72	1.584	337.1	0.244	28
23	1.289	298.9	1.190	203	73	2.032	329.4	0.201	18
24*	1.1	123.7	1.003	45	74	1.345	337.0	1.383	24
25	1.191	342.0	1.322	46	75	1.320	8.9	1.283	88
26	1.1	312.6	0.762	8	76	1.410	38.0	0.279	6
27	1.108	297.2	0.466	62	77	1.565	34.7	0.188	17
28	1.241	350.7	0.461	33	78	1.503	48.7	1.436	3
29	1.1	7.2	0.065	28	79	1.363	43.2	1.436	16
30	1.214	65.7	1.362	2	80	1.198	37.7	0.665	23
31	1.649	319.3	0.072	52	81	1.368	35.1	1.381	30
32	1.1	44.1	0.927	20	82	1.491	310.3	1.020	9
33	1.538	329.9	0.041	9	83	1.670	313.6	1.016	1
34	1.560	337.2	0.045	2	84	1.518	9.9	1.276	28
35	1.147	316.8	0.813	6	85	1.599	27.7	0.225	7
36*	1.147	255.1	1.046	7	86	1.648	44.5	1.577	30
37	1.828	320.8	0.085	2	87	1.754	24.7	0.317	15
38	1.406	316.4	0.664	1	88	1.858	20.9	0.441	36
39	1.202	62.6	0.743	19	89	1.442	320.5	0.874	43
40	1.868	326.7	0.133	49	90	1.558	326.2	0.943	15
41	1.876	332.8	0.127	10	91	1.752	33.7	0.121	31
42	1.1	1.0	1.167	8	92	1.849	316.5	1.027	26
43	1.476	343.9	0.085	3	93	1.489	4.3	1.141	5
44	1.1	23.7	0.714	4	94	2.063	14.0	0.068	15
45	1.248	27.7	1.584	34	95	1.435	334.9	1.200	41
46	1.288	57.3	1.330	6	96	1.403	334.2	1.563	8
47*	1.1	214.9	1.522	11	97	1.620	37.7	1.543	3
48	1.325	347.3	1.228	43	98*	1.1	157.6	0.060	28
49	1.1	12.1	0.979	7	99	1.947	334.3	0.308	12
50	1.298	250.2	0.269	19	100	1.313	44.5	1.128	4

* Particle captured in the rear side of the fiber.
** Denotes the number of generated particles from the full particle generation plane in Figure 1.

Table 4. Simulation Result of Dendrites Growth on Fiber for the Case of Pe = 5000 and R = 0.1

M	r	θ	z	N*	M	r	θ	z	N*
1	1.1	280.3	1.358	226	38	1.967	22.9	1.578	33
2	1.1	63.4	1.393	146	39	1.341	18.2	1.530	44
3	1.102	286.8	1.514	402	40	2.079	19.6	1.463	113
4	1.1	316.9	1.570	144	41	1.303	33.0	0.501	30
5	1.270	320.2	1.489	88	42	1.628	350.5	0.089	23
6	1.161	53.8	1.418	209	43	1.194	15.6	1.095	14
7	1.1	43.5	0.597	195	44	1.887	351.6	1.513	57
8	1.228	340.4	1.573	77	45	1.472	39.2	0.320	32
9	1.1	15.0	0.528	18	46	1.349	24.6	0.469	7
10	1.271	46.2	1.381	150	47	1.444	22.1	0.330	13
11	1.203	23.6	1.448	39	48	2.109	340.3	0.308	26
12	1.1	332.8	1.204	68	49	1.982	341.6	0.467	22
13	1.309	331.4	0.057	169	50	1.526	347.7	1.188	51
14	1.566	337.3	0.048	183	51	2.384	350.0	0.361	42
15	1.322	347.0	1.476	94	52	2.313	345.8	0.102	59
16	1.820	339.7	0.128	48	53	2.574	348.8	0.323	32
17	1.1	331.0	0.291	20	54	1.372	32.5	0.745	30
18	1.924	342.3	0.276	58	55	1.483	18.7	0.528	20
19	1.768	23.6	1.585	54	56	1.477	11.1	0.256	2
20	1.1	342.5	1.063	10	57	1.498	16.7	1.413	34
21	1.247	41.5	0.468	4	58	2.763	348.5	0.263	25
22	1.949	348.5	0.013	20	59	1.541	13.6	1.236	42
23	2.040	350.7	0.174	24	60	1.568	9.9	1.064	24
24	1.343	39.6	0.637	2	61	1.657	8.3	0.215	16
25	1.165	352.1	1.067	5	62	1.488	26.1	0.773	11
26	1.357	350.4	1.106	34	63	2.023	355.9	1.514	15
27	1.1	23.5	1.017	7	64	2.253	17.1	1.437	50
28	1.305	341.5	0.064	12	65	2.505	345.3	0.051	22
29	2.122	345.8	0.042	62	66	1.746	12.9	1.093	6
30	1.278	37.8	0.287	21	67	1.918	14.7	1.178	25
31	1.523	36.4	0.599	84	68	2.455	354.4	0.340	8
32	1.209	10.5	0.387	10	69	2.185	353.2	1.580	16
33	1.303	324.5	1.317	34	70	2.067	11.4	1.108	9
34	1.153	14.8	1.517	3	71	2.567	355.8	0.186	65
35	2.224	349.7	0.242	6	72	2.518	351.2	0.501	4
36	1.448	347.3	0.086	72	73	2.353	13.1	1.371	38
37	1.298	7.8	0.218	45					

* Denotes the number of generated particles from the full particle generation plane in Figure 1.

Z_2 were made relatively free of end effects since dedrites were also allowed to flourish in the buffer regions. As a result, no evident difference was detected between Z_2 = 0.8 and 1.6, as seen from the table. Judging from these considerations, values of $\Delta\tau$ = 0.5 and Z_2 = 1.6 were adopted in this investigation.

A flow chart of the computational procedure is given in Figure 2. The present model implicitly made use of the following assumptions:

1) Existence of dendrites on the fiber has an insignificant effect in the flow field around the fiber.

2) Spatial and time distribution of incoming particles are random microscopically, and no new particle will enter the cell before the present one is either captured or lost.

3) A particle is always captured when it collides on the fiber surface or with any previously captured particles.

4) There is no reentrainment of captured particles or dendrites.

The filtration conditions investigated are listed in Table 2.

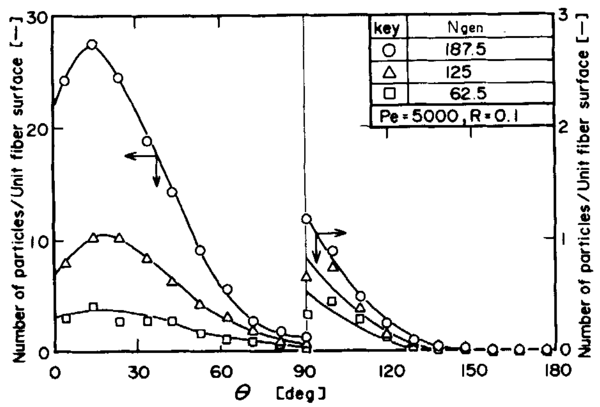

Figure 4. Angular distribution of number of deposited particles on a fiber for the case of Pe = 5,000 and R = 0.1.

SHAPES AND DISTRIBUTION OF DENDRITE

Examples of the simulation results for the cases of Pe = 200, R = 0.1 and Pe = 5,000, R = 0.1 were listed in Tables 3 and 4, respectively. Although particles were captured on the fiber surface in the initial stage of the particle collection, most of the particles were captured by previously captured particles and they formed dendritic agglomerates and grew away from the fiber. It is remarkable that the deposition of particles occurred also on the rear surface of the fiber, for the case of Pe = 200. This kind of deposition of particles cannot happen by other mechanical collection mechanisms. This agreed with experimental observations (Yoshioka et al., 1967) and with Payatakes' model (1979).

Figures 3 and 4 show the average distribution of deposited particles on the fiber surface under various filtration conditions. In these figures, maximum deposition appeared about 20° to 40° away from the front stagnation and it shifted to larger angle as Pe increased. When Brownian movement of particles were dominant compared with convection, i.e., for the case of pure diffusion (Pe = 0), uniform deposition of particles over the entire surface is expected. On the contrary, when convection is dominant, this corresponds to pure interceptional deposition of particles; Kanaoka

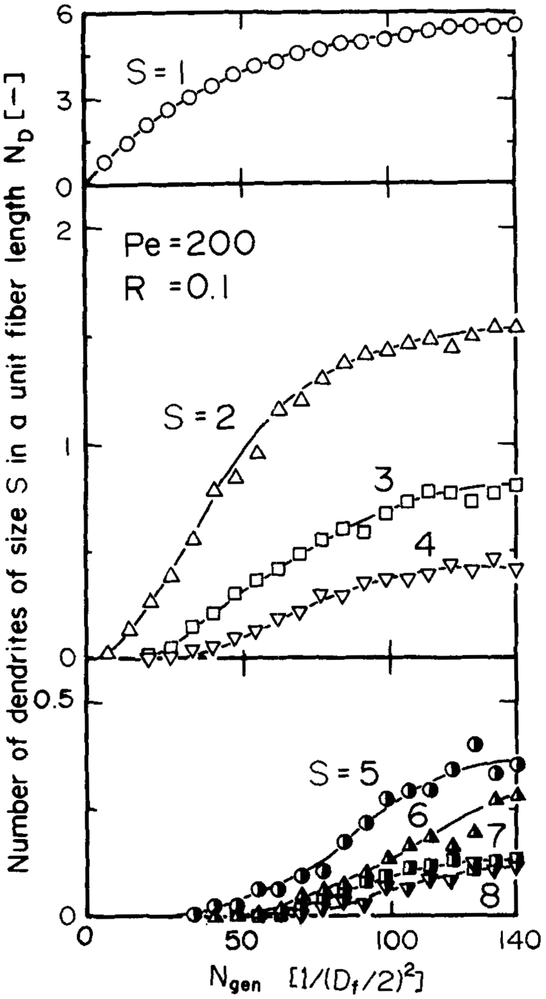

Figure 5. Time dependency of number of dendrites in a unit fiber length for the case of Pe = 200 and R = 0.1.

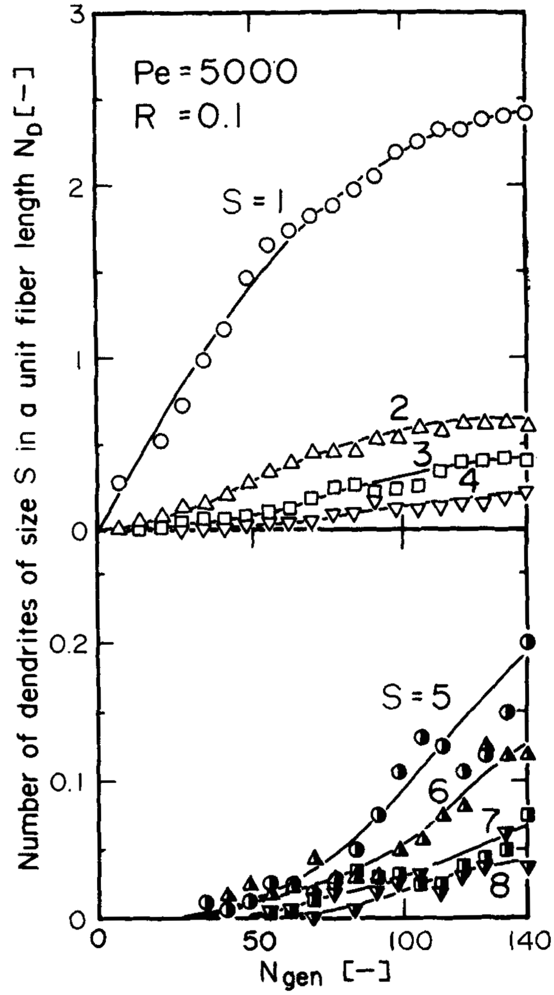

Figure 6. Time dependency of number of dendrites in a unit fiber length for the case of Pe = 5,000 and R = 0.1.

et al. (1980) has shown that the maximum deposition of particles appeared at a certain angle from the front stagnation. Consequently, appearance of a peak around the front stagnation at intermediate Peclet number can be considered as the effect of the convective motion of fluid.

Figures 5 and 6 show the changes in number of dendrites consisted of S particles in a unit fiber length, N_D as a function of number of generated particles from a corresponding generation area to the fiber with a unit length N_{gen}. Although very large dendrites were observed in the simulation, their number was too few statistically and thus they were not shown here. As seen from the figures, N_D increases with N_{gen} regardless of S, but for a given N_{gen}, N_D for the case of $Pe = 200$ is larger than that for $Pe = 5{,}000$. It is also remarkable that N_D of a larger size is always smaller than that of a smaller ones, even if N_{gen} increases as many as 140, which corresponds to the filtration time of about 10^3 and 2.5×10^4 hours for $Pe = 200$ and 5,000, respectively, when 0.5-μm particles are filtrated by a 5-μm fiber. This means that there exist many small-size dendrites even if a fiber is heavily loaded with captured particles.

Figure 7 shows the average dendrite size S_{av} as a function of N_{gen}. Dendrites for the $R = 0.2$ grow faster than that for $R = 0.1$ regardless of Pe; for the same R, average dendrite size does not change much by changing the Peclet number.

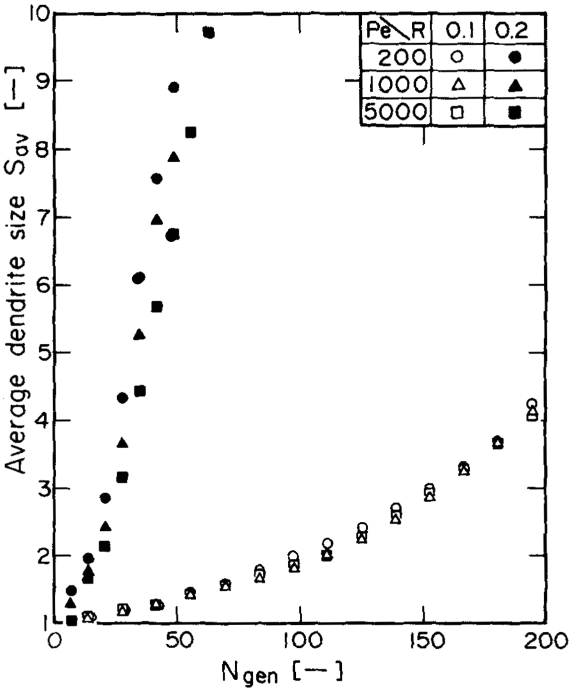

Figure 7. Time dependency of average dendrite size.

COLLECTION EFFICIENCY

The collection efficiency of a dust-loaded fiber with respect to the capture of the Mth particles on a fiber section with a length of

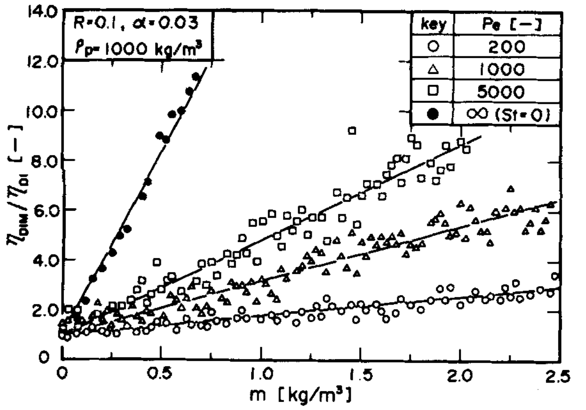

Figure 8. Normalized collection efficiency of a dust-loaded fiber for the case of $R = 0.1$.

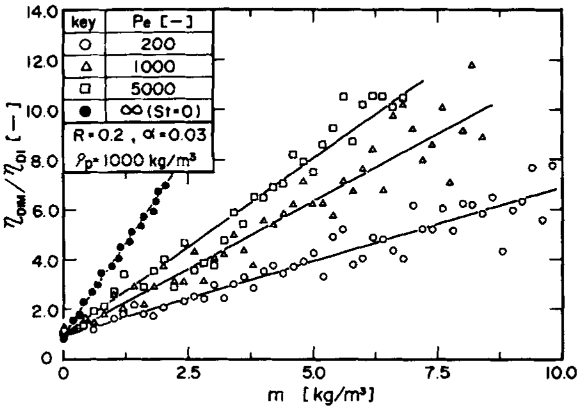

Figure 9. Normalized collection efficiency of a dust-loaded fiber for the case of $R = 0.2$.

$D_f/2$, η_{DIM} is simply given by the following equation (Kanaoka et al., 1980).

$$\eta_{DIM} = 1/N_M \tag{11}$$

where

$$N_M = 1/L \sum_{i=1}^{L} N_{Mi} \tag{12}$$

Here, N_{Mi} is the number of incoming particles between the captures of the Mth and $(M+1)$th particles on the fiber section in the simulation number i.

The accumulated mass of particles deposited in a unit volume of the filter bed m is also related to the number of captured particles M by

$$m = \frac{M(\pi D_p^3/6)\rho_p}{(D_f/2)(\pi D_f^2/4)/\alpha} = \frac{4}{3}\rho_p \alpha R^3 M \tag{13}$$

Figures 8 and 9 show the normalized collection efficiency η_{DIM}/η_{DI} vs. dust load m together with the results for the case of $St = 0$ which corresponds to the case of $Pe = \infty$. Here, is the collection efficiency of a clean fiber, reported by Stechkina (1966). The fact that the values of η_{DIM}/η_{DI} at zero dust load were close to unity in both figures means that the present model yielded reasonable prediction even for a clean fiber. Although η_{DIM}/η_{DI} scatters, it increases nonlinearly with dust load M. To express it by a function of m, they were approximated by Eq. 14, and optimum coefficients and indicies were determined using least mean square method. Obtained values are listed in Tables 5 and 6.

$$\eta_{DIM}/\eta_{DI} = 1 + am^b \tag{14}$$

Obviously, values of b in the equation are close to unity, regardless of Pe and R. Hence, they were approximated by a linear function, Eq. 15, and coefficient λ was determined. They were also listed in Tables 5 and 6 together with the values for the case of $St = 0$.

$$\eta_{DIM}/\eta_{DI} = 1 + \lambda m \tag{15}$$

In the tables, the value of coefficient, collection efficiency raising factor λ, varies from 15 to 0.8 and from 3.1 to 0.6 for $R = 0.1$ and 0.2, respectively, when Pe ranges from infinity to 200. This means that increasing rate of the collection efficiency in large Pe and small R is larger than that in the region of small Pe and large R, where collection efficiency of a clean fiber is high. This trend was also observed for case of inertia-interceptional collection mechanism. Hence it would be said that collection efficiency raising factor could be large, when collection efficiency of a clean fiber is small.

TABLE 5. OPTIMUM VALUES OF a AND b IN EQ. 14 AND λ IN EQ. 15 FOR THE CASE OF $R = 0.1$

Pe	200	1,000	5,000	∞*
a	0.614	2.15	3.84	—
b	1.29	1.03	1.00	—
λ	0.789	2.19	3.84	14.8

* Value given by Kanaoka et al. (1980) at $St = 0$, which is equivalent to $Pe = \infty$ in this work.

TABLE 6. OPTIMUM VALUES a AND b IN EQ. 14 AND λ IN EQ. 15 FOR THE CASE OF $R = 0.2$

Pe	200	1,000	5,000	∞*
a	0.599	1.02	1.13	—
b	0.991	1.03	1.14	—
λ	0.588	1.07	1.42	3.09

* Value given by Kanaoka et al. (1980) at $St = 0$, which is equivalent to $Pe = \infty$ in this work.

ACKNOWLEDGMENT

The authors wish to thank the Fellowship provided in 1980 by The Japan Society for the Promotion of Science through National Research Council of Thailand for Wiwut Tanthapanichakoon to come to Kanazawa University.

NOTATION

$A(t)$	= fluctuating term used in Eq. 1, cm/s
a	= constant used in Eq. 14
b	= constant used in Eq. 14
C_m	= Cunningham's correction term
D_{BM}	= Brownian diffusivity ($=C_m kT/3\pi\mu D_p$), cm²/s
D_f, D_p	= fiber and particle diameters, μm
H, h	= dimensionless half height of generation plane ($=2h/D_f$) and half height of generation plane, cm
k	= Boltzmann constant ($=1.38026 \times 10^{-16}$), erg/K
L	= total simulation number
M	= number of particles captured on a fiber with unit length Z
m	= loaded mass of particles in a unit filter volume, kg/cm³
N_D	= number of dendrites on a fiber with unit length
N_{gen}	= total number of particles generated per unit generation area ($=D_f/2xD_f/2$ in dimensional), L/cm²
N_M	= number of incoming particles between the captures of mth and $(M+1)$th particle
n	= normal standard random vector

P,p = dimensionless particle position vector ($=2p/D_f$) and particle position vector, cm
Pe = Peclet number ($=D_f u_0/D_{BM}$)
R = interception parameter ($=D_p/D_f$)
R_c = dimensionless radius of Kuwabara's cell ($=1/\sqrt{\alpha}$)
r = relative particle position vector, cm
S = dendrite size
St = Stokes number ($=C_m \rho D_p^2 u_0/9\mu D_f$)
T = absolute temperature, K
$t,\Delta t$ = time and time subinterval, s
U, u = dimensionless air velocity vector ($=u/u_0$) and air velocity vector, cm/s
V,v = dimensionless particle velocity vector ($=v/u_0$) and particle velocity vector, cm/s
W = probability function defined in Eq. 3
w = relative particle velocity to air, cm/s
x = x component in a Cartesian coordinate, cm
y = y component in a Cartesian coordinate, cm
Z,z = dimensionless length of a representative fiber ($=2z/D_f$) and length of a representative fiber, cm
z = z component in a Cartesian coordinate, cm

Greek Letters

α = packing density of a filter
β = reciprocal of relaxation time of a particle, s
η = single fiber collection efficiency
θ = angle, deg
κ = hydrodynamic factor
λ = collection efficiency raising factor, m^3/kg
μ = fluid viscosity, g/cm·s
ρ = particle density, g/cm^3
σ = standard deviation of normal standard random number n, cm
$\tau,\Delta\tau$ = dimensionless time ($=2tu_0/D_f$) and dimensionless time subinterval
ψ = stream function of Kuwabara's flow field

Subscripts

D = diffusion
I = interception
i = ith step
M = dust loaded
x = x direction
y = y direction
z = z direction
0 = initial
1,2,3 = number of subsection

LITERATURE CITED

Barot, D. T., C. Tien, and C. S. Wang, "Accumulation of Solid Particles on Single Fibers Exposed to Aerosol Flows," *AIChE J.*, **26**, 289(1980).

Bhutra, S., and A. C. Payatakes, "Experimental Investigation of Dendritic Deposition of Aerosol Particles," *J. Aerosol Sci.*, **10**, 445(1979).

Billings, C. E., "Effect of Particle Accumulation in Aerosol Filtration," Ph.D. Dissertation, Calif. Inst. of Technol., Pasadena, CA (1966).

Chandrasekhar, S., "Stochastic Problems in Physics and Astronomy," *Review of Modern Phys.*, **15**, 1(1943).

Doob, J. L., "The Brownian Movement and Stochastic Equations," *Annals of Mathematics*, **43**, 2(1942).

Kanaoka, C., H. Emi, and T. Myojo, "Simulation of Deposition and Growth of Airborne Particles on a Filter," *Chem. Eng. Ronbunshu*, **5**, 535(1978).

———, ———, ———, and M. Ohta, "Estimation of Collection Efficiency of Air Filter with Dust Load," *Int. Chem. Eng. Symp. Ser.*, No. 59, 3: 4/1(1980).

———, ———, ———, "Simulation of the Growing Process of a Particle Dendrite and Evaluation of a Single Fiber Collection Efficiency with Dust Load," *J. Aerosol Sci.*, **11**, 377(1980).

Kimura, N., and K. Iinoya, "Collection Efficiency of Fiber Mat Filter with Dust Loading," *Kagaku Kogaku* (Chem. Eng. Japan), **28**, 39(1964).

Kuwabara, S., "The Forces Experienced by Randomly Distributed Parallel Circular Cylinders of Spheres in a Viscous Flow at small Reynolds Numbers," *J. Phys. Soc. Japan*, **14**, 527(1957).

Payatakes, A. C., and C. Tien, "Particle Deposition in Fibrous Media with Dendrite-like Pattern. A Preliminary Model," *J. Aerosol Sci.*, **7**, 85(1976a).

———, "Model of Aerosol Particle Deposition in Fibrous Media with Dendrite-like Pattern. Application to Pure Interception during Period of Unhindered Growth," *Filtration and Separation*, **13**, 602(1976b).

———, "Model of the Dynamic Behavior of a Fibrous Filter. Application to the Case of Pure Interception during Period of Unhindered Growth," *Powder Tech.*, **14**, 267(1976c).

———, "Model of Transient Aerosol Particle Deposition in Fibrous Media with Dendritic Pattern," *AIChE J.*, **23**, 192(1977).

———, and L. Gradon, "Dendritic Deposition of Aerosol Particles in Fibrous Media by Inertial Impaction and Interception," *Chem. Eng. Sci.*, **35**, 1083(1980).

———, ———, "Dendritic Deposition of Aerosol by Convective Brownian Diffusion for Small, Intermediate and High Particle Knudsen Numbers," *AIChE J.*, **26**, 443(1980).

Stechkina, I. B., and N. A. Fuchs, "Studies on Fibrous Aerosol Filters. I: Calculation of Diffusional Deposition of Aerosols in Fibrous Filters," *Ann. Occup. Hyg.*, **9**, 59(1966).

Tanthapanichakoon, W., "Stochastic Analysis of an Activated Sludge Wastewater Treatment Plant with Diurnal Random Inputs and Random Process Parameters via Monte Carlo Simulation," Ph.D. Dissertation, Univ. of Texas at Austin (1978).

Tien, C., C. S. Wang, and D. T. Barot, "Chainlike Formation of Particle Deposits in Fluid-particle Separation," *Science*, **193**, 983(1977).

Uhlenbeck, G. E., and L. S. Ornstein, "On the Theory of Brownian Motion," *Phy. Review*, **36**, 3(1930).

Wang, C. S., M. Beizaie, and C. Tien, "Deposition of Solid Particles on a Collector: Formation of a New Theory," *AIChE J.*, **23**, 879(1977).

Wang, M. C., and G. E. Uhlenbeck, "On the Theory of Brownian Motion I," *Review of Modern Physics*, **17**, 2(1945).

Yoshioka, N., H. Emi, and H. Sone, "Experimental Examination of Impaction of Efficiency Aerosol Particles by means of the Single Cylinder," *Kagaku Kogaku* (Chem. Eng. Japan), **31**, 1012(1967).

———, ———, ———, M. Yasunami, and H. Sato, "Filtration of Aerosols through Fibrous Packed Bed with Dust Loading," *ibid.*, **33**, 1013(1969).

Manuscript received April 27, 1982; revision received January 4, and accepted January 24, 1983.